JOURNAL OF MATERIALS SCIENCE 39 (2004) 1249– 1254

Crystalline structure and morphology of a hindered phenol in a chlorinated polyethylene matrix

CHIFEI WU
Institute of Material Science and Technology, East China University of Science and Technology, 130 Meilong-lu, Shanghai 200237, People's Republic of China
E-mail: wucf@ecust.edu.cn

T. KURIYAMA, T. INOUE
Department of Polymer Science and Engineering, Yamagata University, 4-3-16 Jonan, Yonezawa, Yamagata 992-8510, Japan

The crystallization behavior of tetrakis [methylene-3-(3,5-di-*tert*-butyl-4-hydroxyphenyl) propionyloxy] methane (AO-60) in a chlorinated polyethylene (CPE) matrix was investigated. When the AO-60 content is 15 wt%, CPE/AO-60 is an incompatible system. The crystals on the surface of samples changed sequentially from a polyhedron shape to a platelet shape and then to a needle shape as the annealing temperature was reduced. The annealed samples showed two melting peaks. The high temperature peak is due to the melting of the AO-60 crystals observed. In contrast, in the case of a compatible CPE/AO-60 (5 wt%) system, AO-60 crystals also were observed but there was no change in the shape of crystals. The crystal growth of AO-60 within a CPE matrix is thought to depend on the compatibility of CPE/AO-60. © *2004 Kluwer Academic Publishers*

1. Introduction

Tetrakis [methylene-3-(3,5-di-*tert*-butyl-4-hydroxy phenyl)propionyloxy] methane (AO-60) is a very important chemical substance and is one of the most widely used antioxidants for polyolefins. Our attention has been recently focused on the discovery of unknown useful functions of rubbery materials made possible by the addition of hindered phenol compounds such as AO-60 [1–3]. It was found that the addition of hindered phenol compounds caused a novel transition above the glass-transition temperature of a matrix polymer. From both scientific and industrial points of view, this finding is very interesting, because the novel transition enables us to control a wide variety of useful functionalities, such as super damping, shape-memorization, self-adhesiveness and self-restoration [4]. In those cases, the effectiveness of hindered phenol compounds in polymers was found to depend not only on the additive content but also on its molecular aggregation state [5].

It has been well established that AO-60 easily crystallizes in the presence of a solvent [6] or polymer [7, 8]. In addition, the crystallization of AO-60 molecules in a polymeric matrix caused during an aging or heating process can frequently lead to the disappearance of the inherent function as an additive. Hence, the examination of the crystallization of AO-60 is needed.

In our previous studies [5, 9–12], the influence of annealing conditions on the crystallization behavior and dynamic mechanical properties of organic hybrids consisting of chlorinated polyethylene (CPE) and hindered phenol was investigated. These studies were limited to the effects of crystallization of AO-60 on dynamic mechanical properties. However, the influence of the compatibility of CPE/AO-60 on the crystalline structure and morphology of AO-60 has not been studied.

In this study, we selected a CPE having a low molecular weight for enhancing the mobility of AO-60 in the CPE matrix and an AO-60 lot showing a high melting point for easy distinguishment from the melting point of CPE. To determine the relationship between compatibility of CPE/AO-60 and the crystalline structure and morphology of AO-60 formed within a CPE matrix, two kinds of CPE/AO-60 samples with different contents of AO-60 were prepared. We were particularly interested in the effects of the first aggregation state of AO-60 within a CPE matrix on the nucleation and growth of crystals of AO-60.

2. Experimental

2.1. Materials

The CPE used as a matrix in this study, with a chlorination degree of 40 wt%, was a rubbery grade (Daisolac RA140, Daiso Co. Japan). The molecular weight of this grade of CPE was relatively low ($M_n = 1.22 \times 10^4$, $M_w = 2.13 \times 10^5$), and its distribution was broad ($M_w/M_n = 17.5$). AO-60 (chemical structure shown in Fig. 1), which was used as a functional additive, was a commercial antioxidant (ADK STAB AO-60, Asahi Denka Industries Co. Japan).

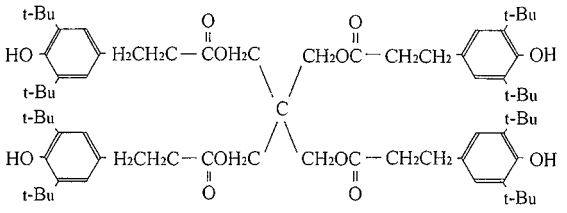

Figure 1 Chemical structure of tetrakis [methylene-3-(3,5-di-*tert*-butyl-4-hydroxyphenyl) propionyloxy] methane, which is abbreviated as AO-60.

AO-60 as a product is a crystalline substance, but AO-60 quenched in an ice-water bath from a temperature higher than its melting point (125°C) is an amorphous substance.

CPE powder was first kneaded using mixing rollers at 50°C for 5 min, and then AO-60 crystalline particles were added to the kneaded CPE, and the mixture was kneaded at 50°C for 10 min. The samples were made molten for 3 min and then pressed in a laboratory hot press at 160°C for 7 min under a pressure of 20 MPa; thereafter, they were cooled to obtain films with a thickness of about 0.5 mm by ice-water quenching. For annealing treatment, the film specimens obtained were immediately placed in a constant temperature chamber at a predetermined temperature and a predetermined time, and they were then quenched in an ice-water bath.

2.2. Dynamic mechanical analysis (DMA)

Dynamic viscoelastic measurements using a dynamic mechanical analyzer (DVE-V4; Rheology Co.) were carried out on sample specimens of the following dimensions; $20 \times 5 \times 1$ mm (length × width × thickness). The temperature dependencies of dynamic tensile moduli were measured at temperatures between −40 and 100°C and at a constant frequency of 11 Hz and a heating rate of 3°C min^{-1}.

2.3. Differential scanning calorimetry (DSC)

DSC measurements were carried out using a DSC-7 Perkin Elmer calorimeter. Samples of about 15 mg in weight and sealed in aluminum were heated from 30 to 160°C at a scanning rate of 20°C min^{-1} under a nitrogen atmosphere.

2.4. Optical microscopic (OM) observation

Samples placed between two cover glasses were observed under a polarizing microscope (OLYMPUS BH-2) with a digital camera (FUJIX HC-300Z/OL) to examine the shape of AO-60 crystals in CPE matrix of various samples.

3. Results and discussion

3.1. Compatibility of untreated CPE/AO-60 sample

The thermal properties of CPE and AO-60 are shown in Fig. 2. The initial AO-60 exhibited a very large melting peak with a maximum at 125°C and enthalpy of fusion

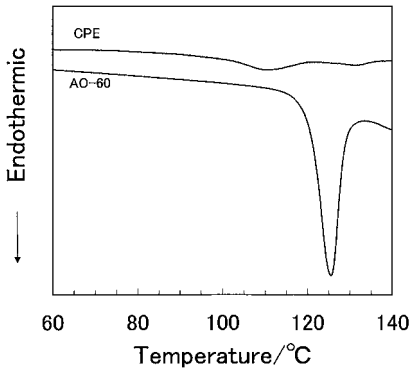

Figure 2 DSC curves of CPE and AO-60. Scan rate was 20°C min^{-1}.

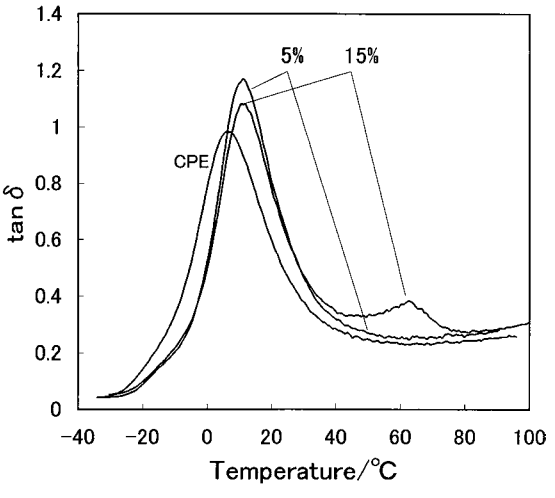

Figure 3 Temperature dependence of loss tangent (tan δ) at 11 Hz for CPE and CPE/AO-60.

$\Delta H = 40$ J/g. In contrast, the melting peak of vitrified AO-60 and annealed amorphous AO-60 disappeared [5]. These results are in good agreement with findings for other hindered phenol substances [8] and they imply that amorphous AO-60 does not easily crystallize in a solid state. On the other hand, the CPE used is a slightly crystallized material. Its melting temperature (T_m) and ΔH are 110°C and 1.2 J/g, respectively.

To elucidate the dispersion states of AO-60 molecules in a CPE matrix, the dynamic mechanical properties were determined. Fig. 3 shows the temperature dependencies of the loss tangent (tan δ) for CPE and two kinds of CPE/AO-60 hybrids. The CPE/AO-60 (5 wt%) sample only showed one tan δ peak, implying that CPE and AO-60 are compatible. In contrast, when the content of AO-60 was 15 wt%, CPE/AO-60 clearly exhibited two peaks, indicating that this sample has two phases (a CPE-rich matrix and an AO-60-rich domain). This two-phase structure was confirmed by an SEM photograph and X-ray microanalysis [2].

3.2. Crystallization of an incompatible CPE/AO-60 system

Fig. 4 shows polarized optical micrographs of CPE/AO-60 (15 wt%) annealed at various temperatures for 4 h. The untreated sample slightly crystallized, the crystals being nonuniform in shape. In contrast, for annealed samples, the crystals observed exhibited various

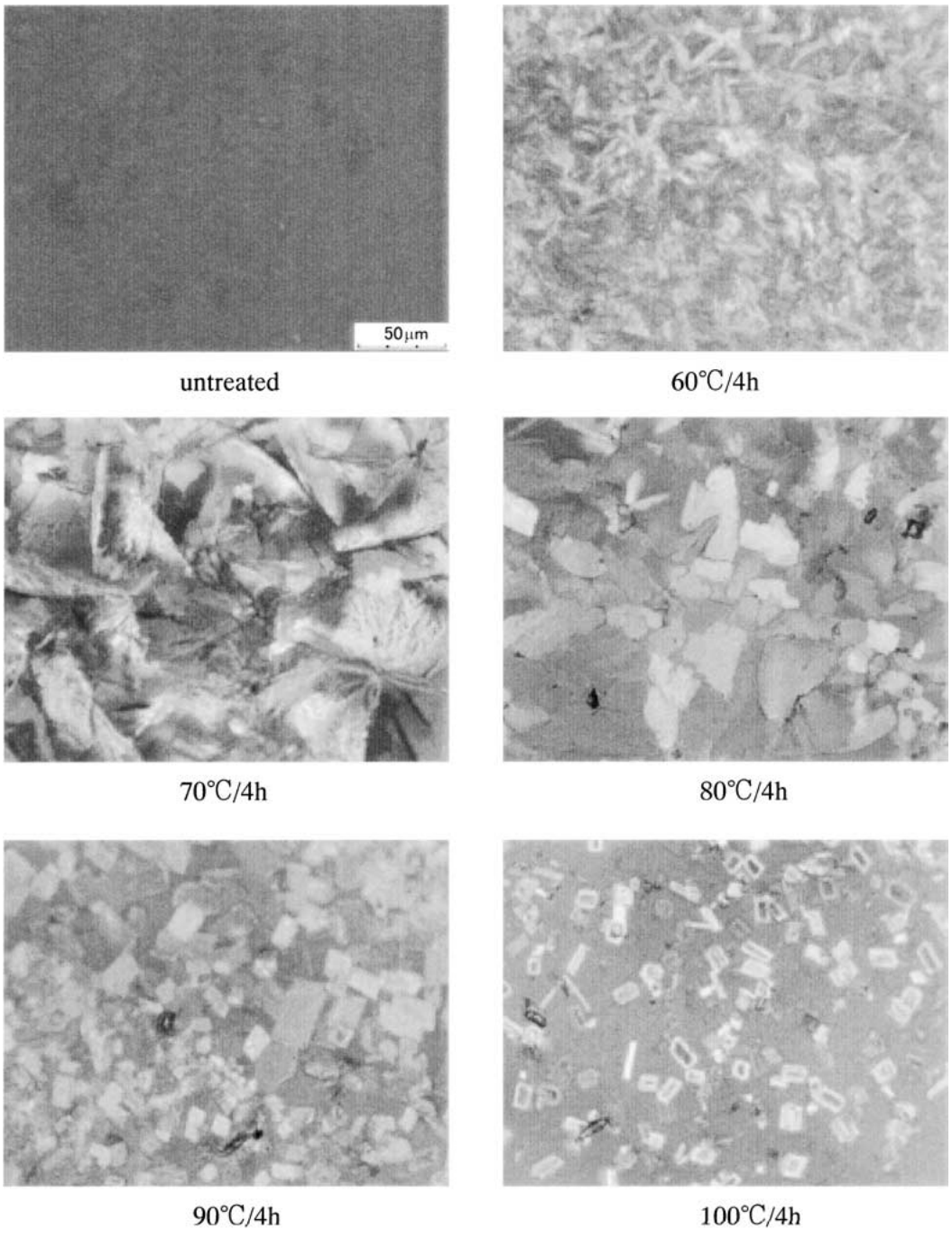

Figure 4 Polarized light micrographs of untreated and various annealed CPE/AO-60 (15 wt%) samples.

shapes. These crystals are attributed to AO-60 because AO-60 molecules crystallize more easily than CPE. As can be seen in Fig. 4, the crystals formed at 100°C are hexahedrons (in three dimensions) in which the width of the hexahedron is larger than its depth. When the annealing temperature was reduced to 90°C, the crystals became rectangular platelets (two dimensional) in shape. With further decreases in the annealing temperature, the shapes of the crystals became irregular. Such change in the growth form of a crystal is attributed to a change in the crystal habit. This character is very different from that of AO-60 crystals (needle-shaped) formed in a dilute solution.

In general, the growth form of a crystal of a certain substance depends on the way in which this substance is supplied from the environmental phase during the process of crystal growth. Matsuoka *et al*. [13]

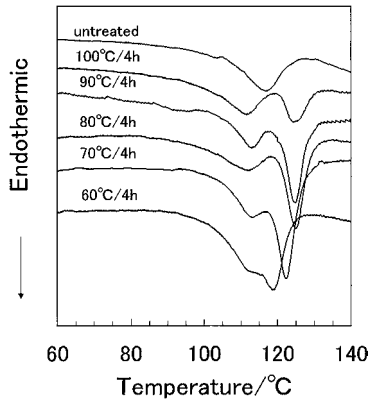

Figure 5 DSC curves of untreated and various annealed CPE/AO-60 (15 wt%) samples. Scan rate was 20°C min^{-1}. The numbers before and after the slanted lines indicate annealing temperature and time, respectively.

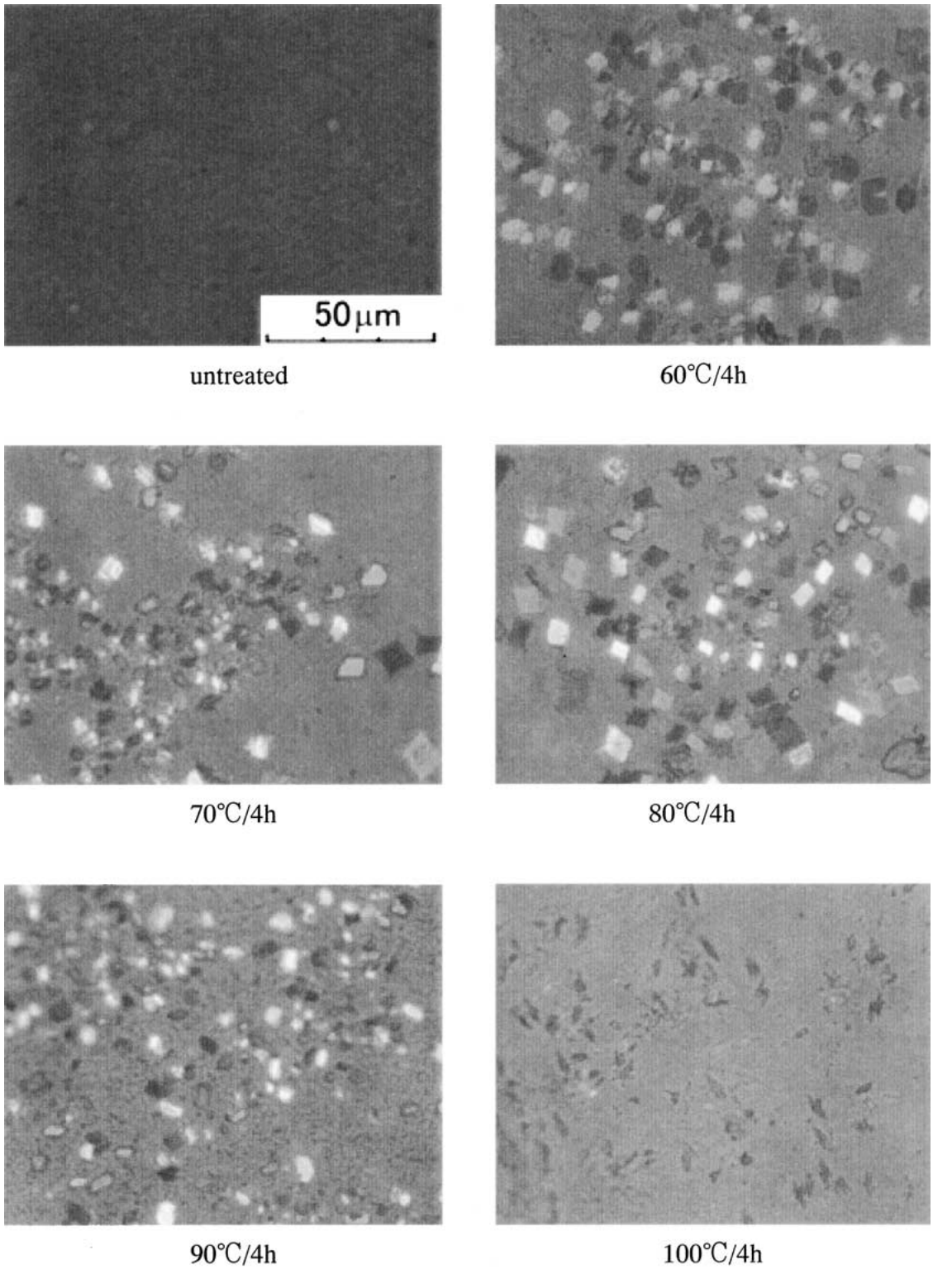

Figure 6 Polarized light micrographs of untreated and various annealed CPE/AO-60 (5 wt%) samples.

extensively investigated the influence of concentration of the crystalline constituent on crystal habit, and they found that a crystal becomes platelet- or needle-shaped when the concentration of the crystalline constituent is low, whereas it becomes a three-dimensional grain shape when the concentration of the crystalline constituent is high. Therefore, a change in the sequential transformation from a polyhedron shape to platelet shape and then to a needle shape of an AO-60 crystal in a CPE matrix may be due to a reduction in the local concentration of AO-60 on the surface of the sample. It is known that the diffusion coefficient of additives obeys the Arrhenius law, as a host polymer has no phase transition in the temperature range of the experiments [8]. Therefore, the reduction in the local concentration of AO-60 on the surface of a sample is reasonable since the transport of AO-60 molecules to the surface decreases as the annealing temperature becomes low.

Fig. 5 shows DSC curves of annealed CPE/AO-60 (15 wt%) hybrids. The untreated sample showed a definite melting peak (117°C). This melting peak is considerably smaller than that of pure AO-60 (125°C,

as shown in Fig. 1) but larger than that of pure CPE (110°C). This was probably caused by the melting of micro-crystals of CPE and imperfect crystals of AO-60 formed during quenching, i.e., the melting peak of 117°C can be considered to be a result of integration of both CPE and AO-60.

In contrast, all annealed samples clearly exhibited two melting peaks. Since these peaks corresponded with those of pure CPE and pure AO-60, they could be attributed to the melting of CPE and AO-60 crystals formed during the quenching process.

Since CPE crystals were not observed in OM, they must be very small micro-crystals. The melting point of a multi-compound system usually depends on blend composition and intermolecular interaction [14]. The first melting peak at low temperatures is invariable regardless of annealing temperature. This implies that there is no intermolecular interaction between CPE and AO-60. In other words, AO-60 molecules were not incorporated into the CPE microcrystals formed at a distinct temperature.

On the other hand, with decreases in annealing temperature down to 80°C, the position of the second melting peak at high temperatures is constant. This also suggests that CPE chains were not incorporated into the AO-60 crystals formed at a distinct temperature and that they are the same in inner structure. However, with further decreases in annealing temperature (down to 70 and 60°C), the second peak shifted to a low temperature. The relatively low melting point is thought to be due to the disorder of the formed AO-60 crystals and/or of the incorporation of the CPE segment into the AO-60-rich domain.

3.3. Crystallization of a compatible CPE/AO-60 system

Fig. 6 shows polarized optical micrographs of CPE/AO-60 (5 wt%) annealed at various temperatures for 4 h. The untreated sample contained relatively small crystals. These small crystals are probably micro-crystals of CPE formed during quenching. In contrast, the crystals formed by annealing at a distinct temperature (except 100°C) are the same in shape and size. This character is very different from crystallization of incompatible CPE/AO-60 (15 wt%), suggesting that other mechanisms may operate for compatible CPE/AO-60 (5 wt%).

Fig. 7 shows DSC curves of annealed CPE/AO-60 (5 wt%) hybrids. All samples, including the untreated sample, showed a melting peak. A comparison with the results shown in Fig. 3 shows that the melting temperatures of annealed CPE/AO-60 (5 wt%) and pure CPE are the same. Thus, it is reasonable to assume that the crystals observed in Fig. 6 are crystals of CPE.

To verify this assumption, we examined the chemical structure and mobility of CPE chains. Formation of large crystals from ethylene segments is impossible because the length of the ethylene section is relatively short, even if CPE can be considered as a block copolymer of ethylene and vinyl chloride. To form larger crystals, other ethylene segments must have very high

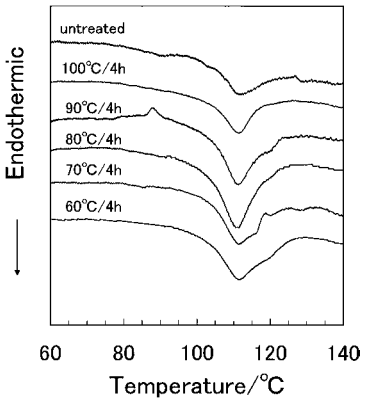

Figure 7 DSC curves of untreated and various annealed CPE/AO-60 (5 wt%) samples. Scan rate was 20°C min^{-1}. The numbers before and after the slanted lines indicate annealing temperature and time, respectively.

mobility. As can be seen in Fig. 2, the addition of 5 wt% AO-60 caused not only an increase in the height of the tan δ peak but also a shift in the position of the tan δ peak. The glass-transition temperature of matrix CPE implies that the AO-60 additive is an antiplasticiter, that is, the mobility of the CPE chains is restricted compared with that of pure CPE. This is conceivable because the intermolecular hydrogen bond between CPE and AO-60[1] is stronger than the interaction of CPE chains. Therefore, crystal growth of CPE in a CPE/AO-60 system is more difficult than in pure CPE. Consequently, the larger crystals shown in Fig. 6 are not CPE crystals.

If the larger crystals shown in Fig. 6 are AO-60 crystals, this hypothesis can be substantiated by an etching experiment of the crystals on the sample surface. While CPE cannot be dissolved in methanol, AO-80 is soluble in methanol. Fig. 8 shows a polarized optical micrograph of CPE/AO-60 (5 wt%) annealed at 80°C for 4 h and then etched by methanol. As can be seen in the figure, the crystals of AO-60 were dissolved by methanol, but their marks were left. Therefore, the crystals shown in Fig. 6 can be assumed to be crystals of AO-60. In addition, the drop in the melting temperature of AO-60 crystals within CPE/AO-60 (5 wt%) annealed at 70 and 60°C for 4 h observed in Figs 2 and 7 may be due to the size of the AO-60 crystals formed and/or the incorporation of the CPE segment. The apparent large crystals of AO-60 shown in Fig. 6 may have been constructed by CPE chains incorporated in the AO-60 micro-crystals.

It is also noteworthy that the crystals of a sample annealed at 100°C for 4 h are very different from those of other samples (see Fig. 6). In this case, the formation of nuclei of crystals is difficult. It is most likely that nuclei of crystals of a sample annealed at 100°C for 4 h are derived from the micro-crystals of CPE. This is because the annealing temperature (100°C) is only slightly below the melting point (110°C) of CPE. In contrast, in the case of an incompatible CPE/AO-60 (15 wt%) system, the nuclei of crystals are thought to be derived from AO-60-rich domains.

A comparison of an incompatible CPE/AO-60 (15 wt%) system and compatible CPE/AO-60 (5 wt%)

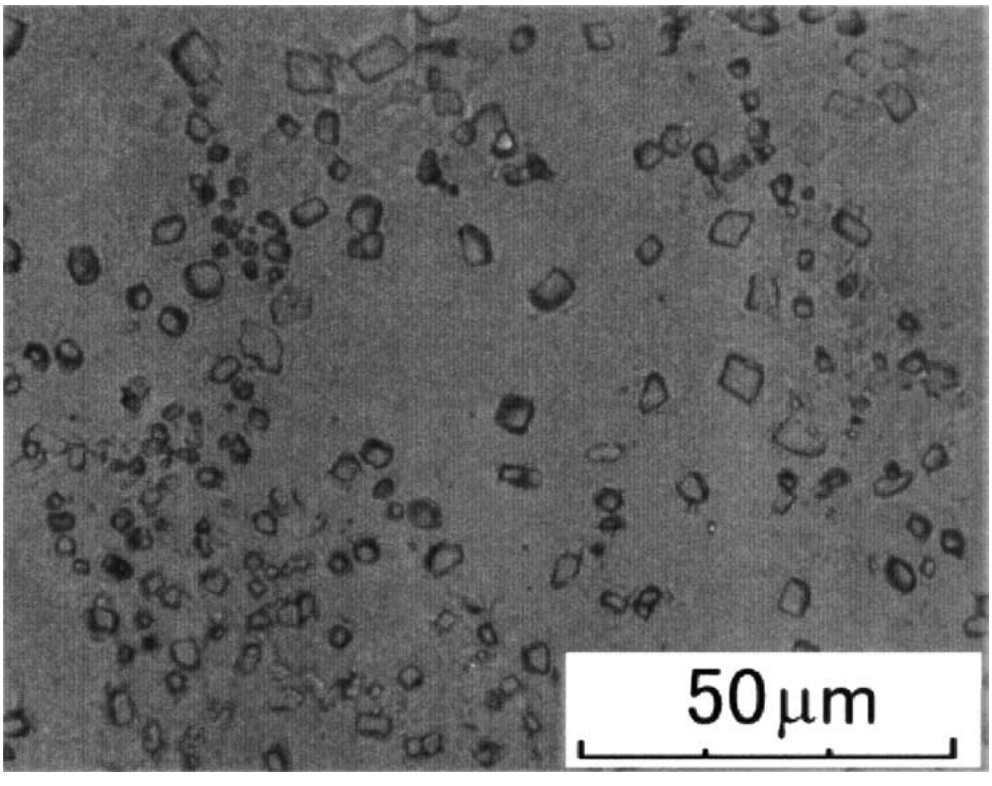

Figure 8 Polarized light micrographs of CPE/AO-60 (5 wt%) annealed at 80°C for 4 h and then etched by methanol.

system showed that the shape of crystals of the former changed but the shape of crystals of the latter remains the same. This difference in crystal growth may be due to the way AO-60 is supplied from the CPE matrix. For the former, AO-60 molecules were supplied as AO-60-rich domains and/or single AO-60 molecules, whereas AO-60 molecules were supplied for the latter.

Finally, it should be stressed that the results obtained in this study are very useful for plastic in which AO-60 is used as an antioxidant. Antioxidants such as AO-60 are often added for inhibiting oxidization of polymers at the time of processing and during service. In the case of polyolefins, the compatibility with AO-60 is lower than CPE, implying that AO-60 molecules distribute in a matrix polymer crystallize more easily. Therefore, the prevention of crystallization of an antioxidant within a matrix polymer is very important, and improvements, such as increasing the molecular weight of the antioxidants, are needed [15].

4. Conclusions

The crystallization of AO-60 molecules distributed in a CPE matrix was investigated. It was found that the crystalline structure and morphology of AO-60 molecules were governed by the annealing condition and the initial dispersion states of the molecules. When the AO-60 content is 15 wt%, CPE/AO-60 is an incompatible system. The crystals on the surface of a sample changed sequentially from a polyhedron shape to a platelet shape and then to a needle shape as the annealing temperature was reduced. The untreated sample showed one melting peak, whereas the annealed samples showed two melting peaks. The second peak at a high temperature is due to the melting of the AO-60 crystals observed. In contrast, in the case of a compatible CPE/AO-60 (5 wt%) system, AO-60 crystals also were observed but there is no change in the shape of crystals. The crystal growth of AO-60 within a CPE matrix is thought to depend on the compatibility of CPE/AO-60. The results obtained in this study are very useful for plastic in which AO-60 is used as an antioxidant.

References

1. C.-F. WU, *J. Mater. Sci. Lett.* **20** (2001) 1389.
2. C.-F. WU, T. YAMAGISHI, Y. NAKAMOTO, S. ISHIDA, S. KUBOTA and K. NITTA, *J. Polym. Sci., Part B: Polym. Phys.* **38** (2000) 1496.
3. C.-F. WU, T. YAMAGISHI, Y. NAKAMOTO, S. ISHIDA, K. NITTA and S. KUBOTA, *ibid.* **38** (2000) 2285.
4. C.-F. WU, *Chin. J. Polym. Sci.* **19** (2001) 445.
5. C.-F. WU, K. MORI, Y. OTANI, N. NAMIKI and H. EMI, *Polymer* **42** (2001) 8289.
6. H. HASUI, T. FURUHATA, K. TAKANASHI and M. OMORI, *Jpn. Patent.* 1985-13018.
7. E. FOLDES and B. TURCSANYI, *J. Appl. Polym. Sci.* **46** (1992) 507.
8. E. FOLDES and J. LOHMEIJER, *ibid.* **65** (1997) 761.
9. C.-F. WU and K. NITTA, *Kobunshi ronbunshu* **57** (2000) 449.
10. C.-F. WU, T. YAMAGISHI, Y. NAKAMOTO and S. ISHIDA, *Polym. Int.* **50** (2001) 1095.
11. C.-F. WU, *Polymer* **44** (2003) 1697.
12. C.-F. WU and S. AKIYAMA, *Polym. J.* **34** (2002) 847.
13. M. MATSUOKA and J. GARSIDE, *J. Crystal Growth* **99** (1990) 1138.
14. P. J. FLORY, "Principles of Polymer Chemistry" (Cornell University Press, New York, 1953).
15. M. MINAGAWA and K. KIKKAWA, *Makromol. Chem., Makromol. Symp.* **70/71** (1993) 433.

Received 14 April
and accepted 14 August 2003